

***Final Draft***  
**of the original manuscript:**

Machatschek, R.; Saretia, S.; Lendlein, A.:

**The interplay between network morphology and degradation kinetics of polymers: Theoretical and experimental analysis by means of a 2D model system.**

In: MRS Advances . Vol. 5 (2020) 11 - 12, 679 - 691.

First published online by Cambridge University Press: 09.12.2019

DOI: 10.1557/adv.2019.457

<https://dx.doi.org/10.1557/adv.2019.457>

# The interplay between network morphology and degradation kinetics of polymers: Theoretical and experimental analysis by means of a 2D model system

Rainhard Machatschek<sup>1</sup>, Shivam Saretia<sup>1,2</sup>, Andreas Lendlein<sup>1,2\*</sup>

<sup>1</sup> Institute of Biomaterial Science, Helmholtz-Zentrum Geesthacht and Berlin-Brandenburg Center for Regenerative Therapies, Kantstraße 55, 14513 Teltow, Germany

<sup>2</sup> Institute of Chemistry, University of Potsdam, Karl-Liebknecht-Straße 24-25, 14469 Potsdam, Germany

\*Correspondence to: Andreas Lendlein

E-mail: andreas.lendlein@hzg.de

## ABSTRACT

*Network formation by cross-linking is a common method to incorporate functions like elastic deformability, shape-memory capability or hydrogel formation into polymer materials for medical applications. Since these materials are often intended to degrade, their design would benefit from a quantitative prediction of the interdependence between network architecture and degradation behavior. Here, we introduce a quantitative description of the degradation behavior of polymer networks. A simplified model was developed under the assumption of having an ideal network, where all network strands are terminated by network nodes and each node is connected to the same number of strands. To describe the degradation of real networks, the model was modified by allowing for a varying connectivity of network nodes, which also included free chain-ends. The models were validated by comparison with Langmuir monolayer degradation data from 2D networks formed by cross-linking oligo( $\epsilon$ -caprolactone)diols with dialdehydes. We found that both the ideal network hypothesis and the real network model were in excellent agreement with the experimental data, with the ideal network hypothesis requiring longer network strands than the real network to result in the same degradation behavior. The models were further used to calculate the degradation curves of the corresponding, non cross-linked molecules. By comparison, it was found that the network formation increases the time required to reach 50% degradation of oligo( $\epsilon$ -caprolactone)diols by only 20%. This difference mainly arises from attaching free chain ends to network points.*

## INTRODUCTION

Improving the state of the art of treatments in regenerative medicine demands for materials that are capable of accomplishing multiple tasks [1]. For example, a material could be designed to maintain a temporary shape, allowing for insertion through a small incision and then to unfold to provide mechanical support [2]. The material would further be directed to release a drug that helps with the patient's recovery and finally to vanish from the body [3, 4]. Such highly multifunctional materials require distinctly integrated functions. This can be achieved by tailored molecular architectures. Besides joining different building blocks, grafting functional side chains or modifying chain-ends, network formation via chemical cross-linking is a common approach to incorporate the required structural features. Very hydrophilic, cross-linked polymers can take up a lot of water and form hydrogels, whereas polymer networks with the ability to form additional stimuli sensitive cross-links can have shape-memory capability [5]. The effect of the shape-memory capability, most probably a shape-shift, would be triggered by an external stimulus. Quite often, the different functions are not orthogonal, but sequentially coupled in a sense that one environmental interaction can trigger multiple functionalities. Moreover, there can be function-function interdependences [6]. Material degradation has a drastic impact on all material properties and therefore on its associated functions. When degradation takes place in a material with shape-memory capability and the cross-linking density decreases, the shape recovery capability is likely to decline [7]. On the other hand, increasing the density of cross-links by means of synthesis is expected to reduce the degradation rate of a material [8]. The development of materials incorporating functions like water uptake, drug release, or shape memory behavior in combination with water uptake could substantially benefit from a predictive model for the interdependence between network morphology and degradation behavior. Such a theoretical model requires comparison with experimental data for the purpose of verification and the determination of the crucial input parameters. Degradation experiments with bulk materials are often not very conclusive in regard to molecular mechanisms, because reaction rates and mass loss behavior are strongly affected by the diffusive transport of reactants and reaction products [9].

The Langmuir monolayer degradation technique has been established to overcome this problem. By combining the appropriate kinetic models with monolayer degradation experiments, an efficient predictive tool for the interdependence of molecular architecture and degradation behavior of macromolecules is available [10]. In a monolayer at the air-water interface, diffusion of reactants and reaction products can be neglected, and the molecular degradation mechanism becomes observable. Typically, to carry out such an experiment, the molecules are spread from dilute solution in a volatile solvent. After evaporation of the solvent, the layer is compressed to a target surface pressure, which is commonly chosen in a way that the compressibility modulus  $\frac{1}{\kappa} = -A_{trough} * \frac{d\pi}{dA_{trough}}$  has a maximum. This ensures that fluctuations of the surface pressure caused by external perturbations have minimal impact on the surface area. The degradation of the macromolecules is carried out under isobaric conditions, which is identified as a constant areal concentration of repeat units. When short, water soluble fragments are dissolved, a reduction of the areal concentration is counterbalanced by compression of the film. The outcome of the experiment is a surface area vs. time curve. This straightforward approach does not work for polymer networks, which keep their shape instead of spreading out and covering large areas. To carry out degradation experiments on 2D polymer networks, these networks have to be prepared in situ, which represents a great challenge. Recently, the reversible formation of biodegradable 2D networks at the air-water interface has been

demonstrated [11]. The network formation was achieved by reacting monolayers oligo( $\epsilon$ -caprolactone) diols (OCL)s and cross-shaped oligo( $\epsilon$ -caprolactone) tetrols with glyoxal. The water soluble dialdehyde glyoxal can react with the hydroxyl groups at the chain-ends to form hemi-acetals and acetals. Each dialdehyde molecule can connect up to four chain-ends upon formation of acetal groups, resulting in the formation of a 2D network. The enzymatically catalyzed degradation of these networks was substantially slower than the degradation of the non cross-linked molecules.

In this work, the experimental degradation curves are evaluated quantitatively by means of a mechanistic model of the degradation of 2D networks, which is derived for that purpose. In the model, the dissolution of 2D networks is divided into two parts. The first part is a statistical consideration of the fragment size distribution. The fragment size distribution depends on the degree of bond dissociation, ranging from 0 to 1, and the architecture of the network. Here, the network architecture was considered as a function of the average connectivity of the nodes, the average strand length and the molar fraction of nodes. The second part encompasses the calculation of the degree of bond dissociation, which contains all information about the time dependence of the dissolution of the network. This number is calculated according to the solution of the differential equations describing the chemical reactions leading to cleavage of bonds in the chain backbones. The comparison between experimental data, fit results and extrapolated degradation behavior in the absence of cross-links is used to demonstrate the impact of cross-linking on the degradation behavior of polymer materials.

## MATERIALS

The preparation of the cross-shaped OCLs was reported in ref [12]. Oligo( $\epsilon$ -caprolactone) diol (OCL diol, trade name CAPA 2304, Solvay Caprolactones, Warrington, U.K.) was used as received. The cross-linker glyoxal was acquired as aqueous solution (40% w/v, Sigma Aldrich, Germany). The characterization data of the linear and cross-shaped OCL materials was reported previously [13]. The lipase from *Pseudomonas cepacia* was purchased from Sigma-Aldrich (Darmstadt, Germany).

## EXPERIMENTS

2D network preparation by cross-linking of OCL diol and OCL tetrol by glyoxal was performed under identical conditions. Preparation and degradation of OCL 2D networks on the air-water interface by Langmuir technique is described in detail elsewhere [11]. Briefly, at  $22 \pm 0.5$  °C, OCL molecules dissolved in chloroform were spread at the air-water interface in a Langmuir trough ("high compression", Biolin Scientific, Espoo, Finland). After 10 minutes of chloroform evaporation, the OCL monolayer is compressed and withheld at the constant surface pressure of  $7 \text{ mN} \cdot \text{m}^{-1}$ . For cross-linking of the OCL hydroxyl end groups, glyoxal was injected into the subphase (glyoxal/caprolactone molar ratio in the subphase = 20 000). After 18 h of reaction time, the lipase was injected into the subphase and the OCL 2D network area reduction due to degradation was recorded. The Lipase concentration in the subphase for degrading the 2D network formed by OCL diols was  $0.007 \text{ mg} \cdot \text{mL}^{-1}$ . For degrading the 2D networks formed by OCL tetrol, a final concentration of  $0.002 \text{ mg} \cdot \text{mL}^{-1}$  lipase was used.

Another experiment was conducted to study the effect of dialdehyde on OCL diol monolayer degradation by acid. Here, it was hypothesized that the dialdehyde would cross-link the monolayer *in situ* during degradation via acetal bond formation. First, the OCL

diol monolayer (non-cross-linked) degradation due to acidic hydrolysis is studied by lowering the pH of the underlying aqueous subphase. To perform this experiment, OCL diol molecules dissolved in chloroform were spread onto the water subphase (pH = 5.7) in the Langmuir trough. After 10 min of chloroform evaporation, OCL diol monolayer was compressed and held at the constant surface pressure of  $7 \text{ mN} \cdot \text{m}^{-1}$ . For lowering the pH of the water subphase to 2.5, hydrochloric acid (37% HCl; Roth, Germany) dissolved in 5 mL water was injected into the subphase (final HCl concentration in aqueous subphase is 3.15 mM, corresponding to pH = 2.5). Then, the *in situ* cross-linking experiment was carried out by injecting glyoxal (glyoxal/caprolactone molar ratio in the subphase = 20000) dissolved in 5 mL water into the subphase just prior to the HCl solution injection.

## THEORETICAL CONSIDERATIONS

Ideal polymer networks can be described by few parameters. It is, however likely that polymer networks prepared from segment forming and crosslinking compounds contain irregularities like side chains formed by non-reacted segment forming compounds or cyclic structures. In an ideal case (see Figure 1 right), were each node is connected to exactly  $n$  network strands, the network architecture is completely defined by either the average number of repeat units per network strand  $d$  (Eq. 2) or  $x_c$ , the ratio between network nodes and network strand repeating units (Eq.1). In addition, to determine the space occupied by or mass contained in the network, the respective spacial requirements or masses of the network nodes and strand repeating units need to be known. In the case of glyoxal cross-linked OCL networks, the maximum connectivity of the network nodes is 4. The minimum connectivity would be one, representing a free chain-end. In the case of  $n=2$  a chain elongation, rather than a network formation, takes place. In reality, the average connectivity  $n$  will be somewhere between 1 and 4 (Figure 1 left). Based on the parameters  $x_c$  and  $n$ , one can derive other numbers which are relevant for the degradation of polymer networks.

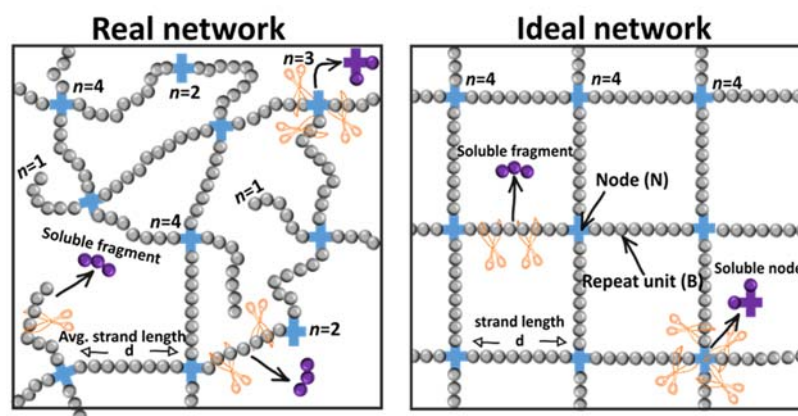


Figure 1: Schematic representation of the degradation of a real network (left) and an ideal network (right). In an ideal network, each strand is terminated by two nodes. The connectivity of the nodes  $n$  is identical for all nodes. To generate water soluble fragments, each strand needs to be cut at least twice. To generate a water soluble node, each of the  $n$  strands surrounding the node needs to be cut close to the node. In a real network, the connectivity of the nodes  $n$  can vary. In addition, there are free chain-ends (connectivity  $n = 1$ ), where soluble fragments can be generated by single chain cuts.

When knowing the ratio between network nodes and repeat units:

$$x_c = \frac{\text{Number of network nodes } (N)}{\text{Number of repeat units } (B)} \quad (1)$$

One can directly deduce the average number of repeating units in a network strand  $d$ :

$$d = \frac{2}{nx_c} \quad (2)$$

The number of network strands  $N_S$ :

$$N_S = \text{number of network strands} = \frac{B}{d} = \frac{Bnx_c}{2} \quad (3)$$

And the number of network nodes  $N_C$ :

$$N_C = \text{number of network nodes} = \frac{2N_S}{n} = Bx_c \quad (4)$$

In the case of OCLs cross-linked with glyoxal via the chain-end, the length of the network strands  $d$  is more accessible than  $x_c$ , because  $d$  is defined by the length of the molecules or arms. In an ideal case, where all nodes are connected to  $n$  strands, the average length of the strands is identical to the chain- or arm-length of the molecules. Then,  $x_c$  reaches its maximum and  $d$  its minimum value:

$$x_{c,ideal} = \frac{2}{n_{ideal}d_{chain}} \quad (5)$$

The dissolution of the networks due to random bond scission is separated into two parts: The dissolution of the strands and the dissolution of the nodes. For "free chains" with two chain-ends and a degree of polymerization of  $n_p$ , the fraction of dissolved repeating units with respect to all units in the chain is given by [14]:

$$\frac{n_{diss}}{n_p} = \beta_x(\alpha) = \frac{\sum_{x=1}^{l_{min}} x \omega_x(\alpha)}{n_p} \quad (6)$$

$$\omega_x(\alpha) = \alpha(1-\alpha)^{x-1} [2 + (n_p - 1 - x)\alpha] \quad (7)$$

Here,  $l_{min}$  is the number of repeat units in the largest water soluble fragment and  $\alpha$  is the probability that a bond between two repeat units is broken. To determine  $l_{min}$ , one can refer to literature data, e.g. mass spectroscopy analysis of degradation data. The degree of bond dissociation arises from an analysis of the bond scission kinetics (see below). In contrast to free chains, network strands have no chain-ends. Every fragment needs to be generated by at least two cuts. The fraction of dissolved repeating units from the network strands is derived from Eq. (6) and (7) by removing the contribution of the chain-ends (proportional to  $\alpha$ ) and replacing  $n_p$  by the strand length  $d$ . The fraction of the dissolved repeating units with respect to all units in the strands is given by:

$$\frac{n_{diss}}{d} = y_x(\alpha) = \frac{\sum_{x=1}^{l_{min}} x \alpha^2 (1-\alpha)^{x-1} (d-1-x)}{d} \quad (8)$$

The area reduction due to dissolution of segments from network strands is given by

$$\Delta A_{segments} = d * N_S * y_x(\alpha) * A_{seg} = B * y_x(\alpha) * A_{seg} \quad (9)$$

The area covered by the film prior to degradation is:

$$A_0 = B * A_{seg} + x_c * B * A_{node} = B * A_{seg} (1 + C_n x_c) \quad (10)$$

Then, the normalized area reduction is given by:

$$\frac{\Delta A_{segments}}{A_0} = \frac{y_x(\alpha)}{1 + C_n x_c} \quad (11)$$

Here, the footprint of the nodes was expressed as a multiple of the footprint of the segments via  $A_{node} = C_n * A_{seg}$ . In principle, Eq. (11) should give a rather accurate description of the area reduction behavior of ideal polymer networks. Since the molar fraction of network nodes is small, they do not contribute substantially to the area of the network. For example, for OCL 2K, only 2.5% of all units in the ideal network are nodes. Nevertheless, an

assessment of the degradation of network nodes is worthwhile, because the reduction of the density of network nodes determines the evolution of the storage modulus of the network. To cut out a network node with no segments attached, all strands connected to the node need to be cut right at the base. The probability that a node with no attached segments is dissolved is therefore  $\alpha^n$  and the number of dissolved nodes is  $N_c \alpha^n$ . Probably, the node can also be cut out with some segments attached. The node is solubilized when a maximum of  $l'$  segments are attached. To cut out a node, all  $n$  strands surrounding the node need to be broken, which occurs with a probability of  $\alpha^n$ . In addition, to attach  $x$  segments to the node, also  $x$  bonds have to be unbroken, which happens with a probability of  $(1 - \alpha)^x$ . Finally, we need to consider how those  $x$  segments can be distributed over the  $n$  strands connected to the node. For example, for a node connected to 4 strands, there are 4 possibilities to cut the strands so that exactly one segment remains attached to the node. In general, the number of options to distribute  $x$  segments over  $n$  strands is given by  $\frac{(n+x-1)!}{(n-x)!x!}$ . The probability for the generation of a cut-out node with a total of  $x$  segments attached is then given by the product of the three factors:

$$p_x(\alpha) = (1 + x)\alpha^n(1 - \alpha)^x \frac{(n+x-1)!}{(n-x)!x!} \quad (12)$$

The number of repeating units attached to a network node is  $\frac{nd}{2}$ . Here, the factor  $\frac{1}{2}$  arises from the fact that strands are always attached to two nodes, meaning that the repeat units in a strand are distributed between two nodes. The fraction of dissolved repeat units  $n_{diss}$  with respect to all repeat units attached to a node is:

$$\frac{n_{diss}}{\frac{nd}{2}} = \delta_x(\alpha) = x_c \sum_{x=1}^{l'} (x) \alpha^n (1 - \alpha)^x \frac{(n+x-1)!}{(n-x)!x!} \quad (13)$$

The area reduction due to dissolution of these segments attached to nodes is given by:

$$\Delta A = B * A_{seg} * x_c * \sum_{x=1}^{l'} (x + C_n) \alpha^n (1 - \alpha)^x \frac{(n+x-1)!}{(n-x)!x!} \quad (14)$$

The area reduction due to dissolution of nodes is the sum of the area reduction due to dissolution of nodes with and without attached segments.

$$\Delta A_{nodes} = A_{seg} * B * \sum_{x=0}^{l'} (x + C_n) \alpha^n (1 - \alpha)^x \frac{(n+x-1)!}{(n-x)!x!} \quad (15)$$

The total normalized area reduction due dissolution of nodes and segments from strands is then given by a combination of Eq. (11) and Eq. (15):

$$\begin{aligned} \frac{\Delta A_{segments} + \Delta A_{nodes}}{A_0} &= 1 - \frac{A(t)}{A_0} \\ &= \frac{1}{1 + C_n x_c} [x_c \sum_{x=0}^{l'} (x + C_n) \alpha^n (1 - \alpha)^x \frac{(n+x-1)!}{(n-x)!x!} + \frac{1}{d} \sum_{x=0}^{l_{min}} x \alpha^2 (1 - \alpha)^{x-1} (d - 1 - x)] \quad (16) \end{aligned}$$

In an ideal case, where each node is connected to exactly  $n$  strands, the network morphology is completely defined by  $x_c$ , and the only additional parameters for the degradation model are the solubility limits  $l$  and  $l'$  as well the area ratio  $C_n$ . Then, Eq. (16) should give an accurate description of the degradation of two-dimensional polymer networks. It is often observed that crosslinking leads to a reduction of the volume of polymers. Also for PCL/glyoxal networks, an area reduction upon cross-linking was found. This observation can be accounted for by choosing a negative value for  $C_n$ . In reality, no network is perfect. With multivalent nodes, there is a high chance that there are free valencies for certain nodes. Moreover, even if the network is formed by connection of chain-ends, as in the case of OCL and glyoxal, there is certainly a fraction of free chain-ends. Real polymer networks are therefore incomplete, and Eq. (16) needs to be adjusted accordingly. The free chain-ends are incorporated rather easily by assuming that only a

certain molar fraction  $\phi$  of all repeat units are part of network strands while a fraction of  $(1-\phi)$  of all repeat units are part of free chainends. Here, network strands are strands connected to two nodes with a connectivity equal or higher than two while chain-ends strands connected to at least one node with a connectivity of one.

$$\phi = \frac{B_{network\ strands}}{B_{chainends} + B_{network\ strands}} = \frac{B_{network\ strands}}{B} \quad (17)$$

$$\frac{(\Delta A_{segments} + \Delta A_{nodes})\phi + (1-\phi)\Delta A_{chainends}}{A_0} = 1 - \frac{A(t)}{A_0} \quad (18)$$

The dissolution of chain-ends in a network is similar to free chains (Eq.7), except that the chain-ends in networks only have one free end and a length of  $d$ .

$$\Delta A_{chainend} = B * A_{seg} * \sum_{x=1}^{l_{min}} x\alpha(1-\alpha)^{x-1}[1 + (d-1-x)] \quad (19)$$

The area occupied by the incomplete network is identical to the area occupied by the complete network, given an identical content of cross-links  $x_c$ . Then, for the network with free chain-ends, the normalized area reduction in dependence on the degree of bond dissociation  $\alpha$  and the molar fraction of repeat units in network strands  $\phi$  is given by combining Eq. (18) and (19):

$$1 - \frac{A(t)}{A_0} =$$

$$\frac{1}{1+x_c C_n} \left\{ \phi x_c \sum_{x=0}^{l'} (C_n + x)\alpha^n (1-\alpha)^x \frac{(n+x-1)!}{(n-1)!x!} + \frac{1}{d} \sum_{x=0}^{l_{min}} x\alpha(1-\alpha)^{x-1} [(1-\phi) + (d-1-x)\alpha] \right\} \quad (20)$$

The values of  $x_c$  and  $n$  for real and ideal networks are connected. The lower the average connectivity of the nodes, the higher the number of nodes required to connect the strands:

$$\frac{x_{c,real}}{x_{c,ideal}} = \frac{n_{ideal}}{n_{real}} \quad (21)$$

For networks formed by connecting chain-ends, i.e. networks formed by OCL and glyoxal,  $x_{c,ideal}$  can be calculated via Equation (5). Then:

$$x_{c,real} = \frac{2}{d_{chain}} * n_{real} \quad (22)$$

We note that there is no equally straightforward way to connect the fraction of repeat units in free chain-ends  $(1-\phi)$  with  $n_{real}$ . This would require to know the distribution of the number of strands per node (see Figure 2).

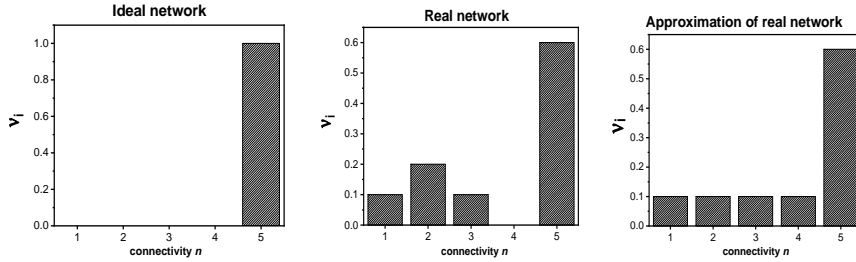


Figure 2: Schematic representation of the distribution of the number of connections per node for a network where each node can undergo a maximum of 5 connections. In the ideal network, all nodes connect exactly  $n_{ideal}$  strands, and the molar fraction of  $v_5$  is 1, whereas all other molar fractions are zero. In a real network, each node can have any number of



connections, resulting in a different molar fraction for each connectivity  $n$ . Here, we make the approximation that all  $v_i$  except for  $v_5$  are identical.  $v_5$  results from the other  $v_i$  via  $\sum_i v_i = 1$ .

For example, when  $n_{ideal}$  is 4 and  $n_{real}$  is 3, there is no way of knowing the fraction of nodes forming chain ends or the fraction of nodes connecting  $n_{ideal}$  strands. Nevertheless, for the distribution of molar fractions  $v_i$  of connectivities  $n_i$ , it is true that:

$$n_{ideal} - n_{real} = \Delta n = (n_{ideal} - 1)v_1 + (n_{ideal} - 2)v_2 + \dots + 0 \quad (23)$$

Here,  $v_1$  is the fraction of chain-ends,  $v_2$  is the fraction of nodes connecting two chains and so on. While the coefficients  $v_i$  are not known, here, we introduce the approximation that they are identical (see Figure 2). Then:

$$v_1 \approx \frac{\Delta n}{(n_{ideal}-1)+(n_{ideal}-2)+\dots+0} \quad (24)$$

For example, for  $n_{ideal} = 4$ , we assume that  $v_1 \approx \frac{\Delta n}{3+2+1} = \frac{\Delta n}{6}$ . Under the approximation explained above, we are able to calculate the molar fraction of repeat units in free chain-ends ( $1 - \phi$ ), which is proportional to  $v_1$ :

$$v_1 * N_c * d = v_1 B x_c * d = v_1 * B * \frac{2}{n_{real}} = B * (1 - \phi) \quad (25)$$

$$(1 - \phi) = \frac{2v_1}{n_{real}} \approx \frac{2 \left( \frac{n_{ideal}-1}{n_{real}} \right)}{(n_{ideal}-1)+(n_{ideal}-2)+\dots+0} \quad (26)$$

With the approximation in Eq. (23), the deviation of the degradation behavior of a non-ideal OCL-glyoxal network from the degradation behavior of an ideal OCL-glyoxal network is completely described by the difference between  $n_{ideal}$  and  $n_{real}$ .

With Eq. (20), which is entirely based on considerations of the probability and size of water soluble fragments, one can calculate the area reduction of the network at any given degree of bond dissociation  $\alpha$ . The calculation of the degree of bond dissociation at any time captures the kinetics of the chemical reactions leading to cleavage of bonds in the network strands. The degradation of OCL, as well as most degradable materials, is based on the chemical reaction of bonds in the chain backbone with water, i.e. hydrolytic cleavage.

At the air-water interface, the water concentration is constant, while the number of cleavable bonds decreases with each successful reaction.

$$\frac{dB}{dt} = -k_{reac} * B \quad (27)$$

Here, the constant  $k_{reac}$  contains all factors that can be considered constant, e.g. the concentration of water or the reaction rate constant. The concentration of catalysts like enzymes or hydroxyl ions can also be considered constant in many cases, while some cases may require to account for a decreasing enzyme activity over time (see below). Equation (27) describes a first order reaction, the solution of which is given by:

$$B(t) = B_0 e^{-k_{reac} t} \quad (28)$$

The degree of bond dissociation  $\alpha$ , i.e. the fraction of broken bonds with respect to all bonds, is given by:

$$\alpha = \frac{B(0)-B(t)}{B(0)} = 1 - e^{-k_{reac} t} \quad (29)$$

Thus, by combining the kinetic equation (29) and the statistical equation (20), the degradation behavior 2D polymer networks can be calculated.

In order to degrade the networks formed *in situ* by cross-linking of OCL diols with a dialdehyde, enzymatic degradation experiments were carried out in solutions containing

glyoxal. It is highly probable that glyoxal reacts with enzymes and reduces their activity. Assuming an exponential decay for the enzymatic activity is a good approximation in case that there is a high excess of dialdehyde.

$$\frac{dB}{dt} = k_{reac} * C_{enz,0} * e^{-s*t} * B \quad (30)$$

Here,  $s$  is the rate constant for the decreasing enzymatic activity. The solution of Eq. (30) is given by:

$$B(t) = B_0 * e^{\frac{k}{s} C_{enz,0} (e^{-s*t} - 1)} \quad (31)$$

$$\alpha = \frac{B(0) - B(t)}{B(0)} = 1 - e^{\frac{k}{s} C_{enz,0} (e^{-s*t} - 1)} \quad (32)$$

## RESULTS AND DISCUSSION

The degradation curve of the OCLs reacting with glyoxal during degradation at pH = 2.5 showed the sigmoid shape typical of a random bond scission mechanism (Figure 3A). Compared to the degradation in the absence of glyoxal, the degradation was notably slower, indicating that indeed, network formation was taking place. The reaction between glyoxal and the chain-ends is an equilibrium reaction that can result in a broad distribution of connectivities for the net points and also take place during degradation. The network created by cross-linking with simultaneous degradation is obviously highly uncontrolled. Nevertheless, the fit curves were identical when assuming a real network (average connectivity  $n$  between 1 and 4) or an ideal network with a connectivity  $n = 4$ . The ideal network assumption resulted in a larger average strand length ( $d = 30, m = 3.400 \frac{g}{mol}$ ) than the real network model ( $d = 23, m = 2600 \frac{g}{mol}$ ). It is intuitive that the tighter network, i.e. the higher the connectivity  $n$  and the shorter the strand length  $d$ , the slower the degradation. The intuition is confirmed by the quantitative model, where the two hypothetical networks, one with higher  $n$  and  $d$ , the other with lower  $n$  and  $d$ , predict the same degradation behavior. The models allow to determine the impact of cross-linking on the degradation of OCLs. To this end, the hypothetical degradation curve, of the corresponding linear molecules, assuming an identical reaction rate constant, was calculated and plotted (grey dotted curves). The simulated degradation curve of linear molecules with a chain length corresponding to the strand length of the hypothetic ideal networks is plotted in each figure. For the linear OCLs, the difference in duration to achieve 50% degradation is only about 20%.

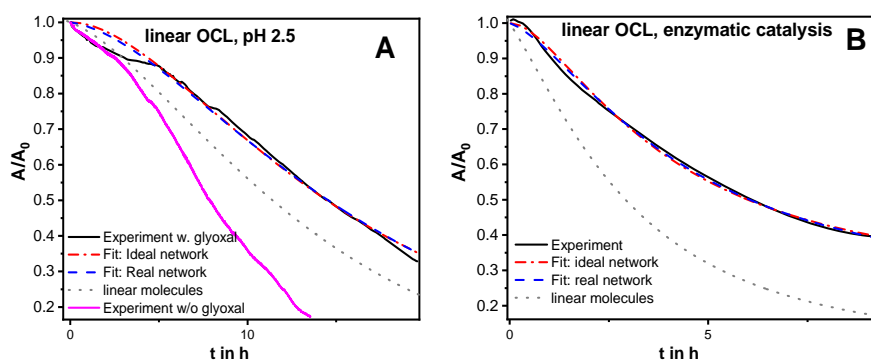


Figure 3: A) Degradation of linear OCL diols reacting with glyoxal during degradation. Network formation and degradation were started at the same timepoint  $t=0$ . B) Enzymatic degradation of networks preformed by linear OCLs. To fit the degradation experiment in the presence of glyoxal at pH 2.5, Eq. (29), (20) and (26) were used. To fit the degradation experiment under enzymatic catalysis, Eq. (32), (20) and (26) were used. For the ideal network fits,  $n$  was set to 4. For the real network fits,  $n$  was allowed to vary freely. The degradation curve of the corresponding linear molecule was calculated using Eq. (6), (7) and (29) for degradation at pH 2.5. For enzymatic catalysis, Eq. (6), (7) and (32) were used to calculate the degradation curve of the corresponding linear molecule. The degree of polymerization of the corresponding molecule and the degradation rate constants were chosen according to the result of the ideal network fit. For all calculations,  $l$  was set to 4 and  $l'$  to 2 where applicable.

When the OCLs were first incubated with glyoxal for 18h and then degraded with enzymes, the shape of the degradation curve was not sigmoidal anymore (Figure 3B). The reason is the deactivation of the enzymes by the dialdehyde in the subphase. Glyoxal is a common cross-linker for proteins and easily reacts with free amine groups, for example in lysine units [15]. Interestingly, this also includes the possibility that the enzymes are incorporated in the network. Since the network forms in an equilibrium reaction, there are always free aldehyde groups that can bind and immobilize enzymes. In principle, enzymes can also become network nodes by linking multiple aldehydes attached to network strands. When accounting for the deactivation of the enzymes, the degradation curve can be fitted equally with the ideal and the real network model. Here, the fits with both models returned the same value for the strand length  $d = 15$  ( $m = 1700 \frac{g}{mol}$ ). This was the minimum strand length allowed for the fit, since the GPC analysis of the linear OCLs suggested that  $d \approx 25$  ( $m = 2800 \frac{g}{mol}$ ). The ideal network assumption with  $n = 4$  returned a degradation rate constant that was about 30% higher than the real network assumption with  $n = 1.5$ . This finding confirms the intuitive assumption that, given an identical bond scission rate, networks with a higher connectivity degrade slower. For the enzymatic degradation, we find a big difference between the degradation behavior of the network, and the hypothetical linear molecule having a length of a network strand  $d$ . Here, the larger difference, compared to the acidic degradation, arises from the deactivation of the enzymes. A system that takes longer to degrade is more affected by the continuous deactivation of the enzymes, and therefore degrades even slower.

The networks formed by cross-shaped OCLs are expected to be closer to ideal network with  $n = 4$  than the networks formed by linear OCLs, since the starting molecules already provide network nodes with  $n = 4$  (See Figure 4, right). According to the GPC analysis,  $d$  was expected to be around 30 ( $m=3600 \text{ g/mol}$ ). Interestingly, the fits of the degradation

curve (Figure 4, left) were identical for the ideal and the real network. That means that the real network model returned a value of  $n = 4$ , albeit with a high uncertainty of  $\pm 3$ .

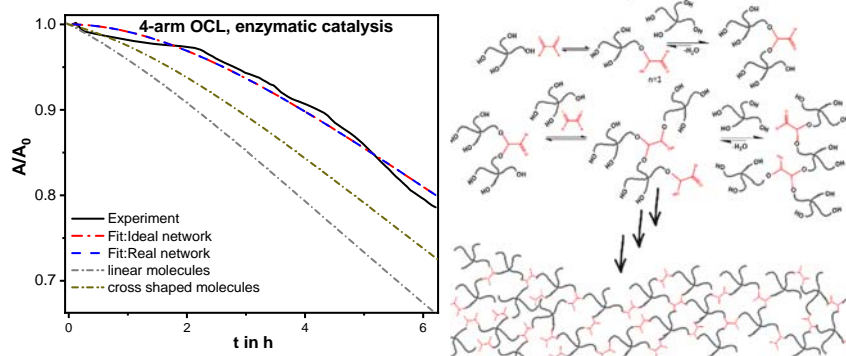


Figure 4: Left: Degradation of networks formed by cross shaped OCL tetrols reacting with glyoxal. To fit the degradation experiment under enzymatic catalysis, Eq. (32), (20) and (26) were used. For the ideal network fits,  $n$  was set to 4. For the real network fits,  $n$  was allowed to vary freely. The degradation curve of the corresponding linear molecule was calculated using Eq. (6), (7) and (32). The degradation curve of the corresponding cross shaped molecule was calculated using Eq. (6), (32) and (7), where “2” was replaced by “1”. The degree of polymerization of the corresponding molecules and the degradation rate constants were chosen according to the result of the ideal network fit. For all calculations,  $l$  was set to 4 and  $l'$  to 2 where applicable. Right: Schematic representation of the network formation upon reaction of cross-shaped OCLs with glyoxal.

For the cross shaped molecules, it makes sense to compare the degradation of the networks with the non cross-linked, cross shaped molecules. The degradation of cross shaped molecules was simulated, based on the hypothesis that cross shaped molecules degrade like linear molecules with only one chain-end, and a degree of polymerization identical to the length of the average length of an arm. With the same rate constants and the strand length returned by the fits ( $d = 40, m = 4560 \frac{g}{mol}$ ), linear molecules degrade faster than cross shaped ones, which degrade faster than networks. The difference, however, is not excessive. There is a distinct difference between the networks formed by the linear OCLs and the cross-shaped molecules. The cross shaped molecules start with an average connectivity of  $(4 \times 1 + 4)/5 = 1.6$ , whereas linear molecules start with a connectivity of 1. The networks formed by cross-shaped molecules are therefore expected to achieve a higher average number of connections per net-point and a lower molar fraction of free chain-ends.

Both for linear and star shaped OCLs, the increase in the average connectivity of the network nodes was achieved by completely reversible reactions. Due to the equilibrium between acetal bonds and free chain ends, there was the possibility that chain-ends, which were generated by the cleavage of ester bonds, reacted with network nodes. In that sense, such a network can be considered as self-healing. The duration of the degradation process (10-20 h) was on the same order as the duration of the network formation (18 h). On the other hand, on the same time-scale, the connectivity of network nodes could have been reduced due to the reaction with water. One could argue that both effects were cancelling, resulting in a network that was well described by an average connectivity  $n$ . However, a self-healing process could have contributed to a steadily decreasing degradation rate (Fig. 3B). Altogether, the networks studied here did not degrade significantly slower than linear molecules. The strong impact of enzyme deactivation on the network degradation is an

artefact of our experimental procedure. It is clear that the networks contained relatively few cross-linkers. In an ideal network with a connectivity of 4, there is only one node per two strands. With a degree of polymerization of about 20 for the strands, there are only 2.5 mol% of cross-linkers. The area covered by the cross-linkers is almost negligible, i.e. the overwhelming majority of area reduction arises from the fragmentation of the strands. The main impact of network formation on the degradation behavior is therefore the removal of free chain-ends. At chain-ends, small and water soluble fragments can be generated by single chain cuts, as opposed to consecutive cuts, which are required to generate water soluble fragments from somewhere in the chain.

Since degradation via random bond scission is a statistical process, a complete description of the degradation of the network can be achieved when the average morphological parameters are known. The parameters, which completely describe the network, are  $d$ ,  $n$  and  $x_c$ . Moreover, these parameters are connected by Eq. (2), meaning that it is sufficient to know only two of them. The cross-linking of chain-ends results in a network with a predefined average length of network strands  $d$ , meaning that the network morphology only depends on the average connectivity  $n$ . For networks prepared by methods where cross-links can be placed at any position in the chain backbone, it is probably more applicable to measure  $x_c$  via spectroscopic methods to achieve the same degree of understanding of the network morphology.

## CONCLUSION AND OUTLOOK

In this work, equations describing the degradation of polymer networks were derived. The main assumption was a statistical cleavage of bonds, with a reaction probability that was independent of the network point density or the location of a bond inside the network. Under this assumption, real networks with free chain-ends, variable network strand length and only partially connected nodes can be described based on averaged parameters for the network architecture. The treatment of real networks was further simplified by assuming that all network node connectivities except for the highest one are realized with equal probability.

The equations describing the area reduction of the network at a given degree of bond dissociation are equally valid for the mass loss of the corresponding three dimensional network at the same degree of bond dissociation. The main difference between two- and three-dimensional systems is diffusion of reactants and degradation products, which complicates the treatment of bulk systems compared to two dimensional ones. For degradable networks that take up a lot of water, e.g. hydrogels, diffusion is probably faster than bond hydrolysis, meaning that degradation would be fully reaction controlled and described by the equations derived above. The recent years have also seen a growing interest in 2D polymers, which are highly defined, synthetic 2D materials [16][17]. Since every atom in these materials is constantly exposed to the environment, degenerative processes are inevitable. The models presented here can serve as a basis for a lifetime prediction of these materials. Future works on the degradation of 2D polymer networks will address the question of the evolution of their mechanical properties during degradation. According to the classical theory of rubber elasticity, the storage modulus of polymer networks is proportional to the network point density. The evolution of the network point density can be easily derived from the equations presented here. To validate the theoretical predictions, the degradation of cross-linked 2D networks will be studied with interfacial rheology.

## ACKNOWLEDGEMENTS

This work was financially supported by the Helmholtz Association through programme-oriented funding and through the Helmholtz Graduate School for Macromolecular Bioscience.

## References

1. P. S. Kowalski, C. Bhattacharya, S. Afeverki and R. Langer, *ACS Biomaterials Science & Engineering* 4 (11), 3809-3817 (2018).
2. G. I. Peterson, A. V. Dobrynin and M. L. Becker, *Advanced Healthcare Materials* 6 (21), 1700694 (2017).
3. A. T. Neffe, B. D. Hanh, S. Steuer and A. Lendlein, *Advanced Materials* 21 (32-33), 3394-3398 (2009).
4. M. C. Serrano, L. Carbajal and G. A. Ameer, *Advanced Materials* 23 (19), 2211-2215 (2011).
5. Y. Osada and A. Matsuda, *Nature* 376 (6537), 219-219 (1995).
6. A. Lendlein, M. Balk, N. A. Tarazona and O. E. C. Gould, *Biomacromolecules* 20 (10), 3627-3640 (2019).
7. C. M. Yakacki, R. Shandas, C. Lanning, B. Rech, A. Eckstein and K. Gall, *Biomaterials* 28 (14), 2255-2263 (2007).
8. D. Darwis, H. Mitomo, T. Enjoji, F. Yoshii and K. Makuuchi, *Polymer Degradation and Stability* 62 (2), 259-265 (1998).
9. K. Sevim and J. Pan, *Acta Biomaterialia* 66, 192-199 (2018).
10. R. Machatschek, B. Schulz and A. Lendlein, *Macromolecular Rapid Communications* 40 (1), 1800611 (2019).
11. S. Saretia, R. Machatschek, B. Schulz and A. Lendlein, *Biomedical Materials* 14 (3), 034103 (2019).
12. J. Zotzmann, M. Behl, D. Hofmann and A. Lendlein, *Advanced Materials* 22 (31), 3424-3429 (2010).
13. A.-C. Schöne, K. Kratz, B. Schulz and A. Lendlein, *Polymer Degradation and Stability* 131, 114-121 (2016).
14. T. Z. Ivanova, I. Panaiotov, F. Boury, J. E. Proust and R. Verger, *Colloid and Polymer Science* 275 (5), 449-457 (1997).
15. M. A. Glomb and V. M. Monnier, *J. Biol. Chem.* 270 (17), 10017-10026 (1995).
16. V. Müller, A. Hinaut, M. Moradi, M. Baljovic, T. A. Jung, P. Shahgaldian, H. Möhwald, G. Hofer, M. Kröger, B. T. King, E. Meyer, T. Glatzel and A. D. Schlüter, *Angew. Chem. Int. Ed.* 57 (33), 10584-10588 (2018).
17. X. Feng and A. D. Schlüter, *Angew. Chem. Int. Ed.* 57 (42), 13748-13763 (2018).